Feedback Linearization Control of Three-Phase UPS Inverter Systems

Dong-Eok Kim, *Student Member, IEEE*, and Dong-Choon Lee, *Member, IEEE*

***Abstract*—In this paper, a feedback linearization technique is proposed to control the output voltage control of three-phase uninterruptible power supply systems. First, a nonlinear model including the output LC filters is derived from the power balance condition between the inverter output terminal and the load side. Then, input–output feedback linearization is applied to the nonlinear model to make it linear. The controller of the linearized model is designed by linear control theory. The tracking control law is obtained with a pole placement technique. It is shown experimentally that the proposed control scheme gives high dynamic responses in response to load variation as well as a zero steady-state error.**

***Index Terms*—Feedback linearization, inverter, LC filters, uninterruptible power supply (UPS).**

I. Introduction

As POWER quality issues become more important for sensitive loads, the uninterruptible power supply (UPS) is becoming more common as a back-up supply for different applications. There are three basic types of UPS systems used in power electronics: offline, line interactive, and online. The line-interactive type is similar to the offline type, but it has the advantage of having a charging battery which functions as an active-power filter [1]. There are also hybrid systems in which an electronic UPS is combined with a rotary UPS, which has large flywheels; these hybrids are often used in various areas of industry [2]. As distributed generation is becoming more common, the UPS is becoming more important not only for enhancing system reliability but also for ensuring power quality in stand-alone generation [1], [3].

The performance of UPS inverters is usually evaluated in terms of the total harmonic distortion (THD) of the output voltage and the transient response. In order to improve these characteristics, a number of control algorithms have been proposed, such as dead-beat, repetitive, proportional resonant, and feedback linearization controllers [1], [4]–[9], and these have achieved relatively good performance. Features of each method are described in [10]. Recently, a new control method was proposed which uses the combined signal information from the filter capacitor and the load currents, measured by one current sensor [11]. One problem with this method is that it is difficult to decide an appropriate share of the turn ratio for the capacitor and load current detection. In [12], a simple control method was proposed to reduce the output impedance by a load current feedback control, which gives more sinusoidal output voltage waveforms for nonlinear loads. However, it has the drawback that its performance is sensitive to parameter variation.

Normally, LC filters are connected to the output terminal of the UPS inverter to attenuate the frequency-related switching voltage harmonics. LC filters are also occasionally used to avoid a negative impact on losses and torque ripple by switching frequency components in motor drives. However, the motor drive uses a current control method, unlike the UPS system which uses a filter capacitor voltage control. Thus, the design of LC filters should differ according to the application. In [13] and [14], a method for designing LC filters was introduced that minimizes a cost function at the expense of increased output impedance. The parameters of LC filters should be determined by considering both the reactive power of the filter and the controller response, which was investigated in [15]. In addition, a resonance problem of LCL filters, which are equivalent to LC filters with inductive loads, was solved with active damping method in [16].

On the other hand, a feedback linearization technique has been applied to control the shunt active power filter [17] and the three-phase three-level neutral-point-clamped boost rectifier [18]. The nonlinear control made it possible to obtain better performance, such as a shorter settling time, little overshoot, and fast tracking of output voltages, than PI controllers provide. In [9], a feedback linearization control for a single-input–single-output (SISO) system combined with PI controllers was proposed for UPS inverters, where the energy storage of the LC filters was neglected.

This paper proposes a novel method of controlling three-phase UPS inverters using feedback linearization for multiinput and multioutput (MIMO) systems which does not measure load currents. First, a nonlinear model of the UPS inverter is derived from an instantaneous power balance of the inverter output terminal and the load side; then, an input–output feedback linearization technique is applied to linearize the nonlinear model. Finally, the controller for the linearized model is designed using linear control theory. The tracking control law is obtained with a pole placement method. We show that the proposed control scheme gives high dynamic responses to load variation as well as a zero steady-state error.

Manuscript received April 15, 2008; revised December 2, 2009. First published January 15, 2010; current version published February 10, 2010. This work was supported by the Ministry of Knowledge and Economy, Korea.

D.-E. Kim is with the Department of Electrical Engineering, University of Washington, Seattle, WA 98195-2500 USA (e-mail: cscotop@hanmail.net).

D.-C. Lee is with the Department of Electrical Engineering, Yeungnam University, Gyeongbuk 712-749, Korea (e-mail: dclee@yu.ac.kr).

Color versions of one or more of the figures in this paper are available online at http://ieeexplore.ieee.org.

Digital Object Identifier 10.1109/TIE.2009.2038404

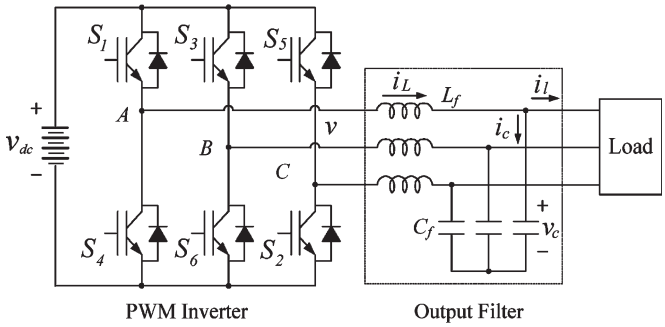

Fig. 1. Three-phase UPS inverter system.

II. Modeling of UPS Inverter Systems

A. Linear Modeling of UPS Inverters

The three-phase UPS system with LC output filters shown in Fig. 1 can be represented in a d–q synchronous reference frame by the following linear model [1]:

$$\dot{i}_d = \frac{1}{L_f} v_d + \omega i_q - \frac{1}{L_f} v_{cd} \tag{1}$$

$$\dot{i}_q = \frac{1}{L_f} v_q - \omega i_d - \frac{1}{L_f} v_{cq} \tag{2}$$

$$\dot{v}_{cd} = \frac{1}{C_f} i_d + \omega v_{cq} - \frac{1}{C_f} i_{ld} \tag{3}$$

$$\dot{v}_{cq} = \frac{1}{C_f} i_q - \omega v_{cd} - \frac{1}{C_f} i_{lq} \tag{4}$$

where L_f is the filter inductance, C_f is the filter capacitance, v_d and v_q are the d–q-axis inverter output voltages, v_{cd} and v_{cq} are the d–q-axis capacitor voltages, i_d and i_q are the d–q-axis inverter output currents, i_{ld} and i_{lq} are the d–q-axis load currents, and ω is the source angle frequency.

B. Power Balance of LC Filters

The terminology used in this section is based on instantaneous power theory [19]. Instantaneous power theory, or "p–q theory," is valid for the analysis and control of electric power systems and active power filters not only in the steady state but also in the transient state.

Fig. 2 shows a per-phase equivalent circuit of UPS inverters with LC filters, where the output voltage of the inverter is assumed to be a sinusoidal voltage source and two cases of the load (resistive and diode rectifier) are considered. The symbol "vai" in Fig. 3 refers to the unit "Volt-Ampere Imaginary," which is to be distinguished from the symbol "var" [19]. The instantaneous real power at each terminal can be expressed as follows:

$$p_{\text{inv\_out}} = \frac{3}{2}(v_d i_d + v_q i_q) \tag{5}$$

$$p_{Lo} = p_{\text{inv\_out}} - p_{L_f} \tag{6}$$

$$p_{Co} = p_{Lo} - p_{C_f} \tag{7}$$

where

$$p_{L_f} = \frac{3}{2} L_f (\dot{i}_d i_d + \dot{i}_q i_q) \quad p_{C_f} = \frac{3}{2} C_f (\dot{v}_{cd} v_{cd} + \dot{v}_{cq} v_{cq})$$

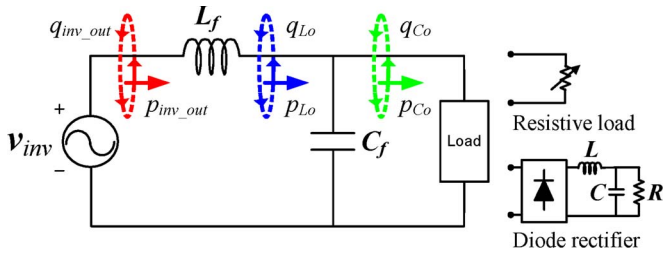

Fig. 2. Per-phase equivalent circuit of LC filters.

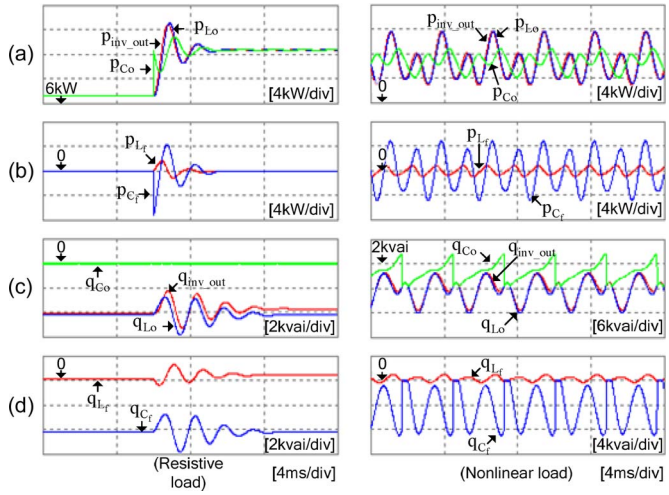

Fig. 3. Instantaneous power variation in LC filters (left: resistive load; right: nonlinear load). (a) Real power at each terminal. (b) Real power of L_f and C_f. (c) Imaginary power at each terminal. (d) Imaginary power of L_f and C_f.

and $p_{\text{inv\_out}}$, p_{Lo}, and p_{Co} are the values of the instantaneous real power at the inverter output terminal, after being filtered by L_f, and after being filtered by C_f, respectively. In addition, p_{Lf} and p_{Cf} are the values of the instantaneous real power trapped in L_f and C_f, respectively. Likewise, the instantaneous imaginary power can be expressed as

$$q_{\text{inv\_out}} = \frac{3}{2}(v_q i_d - v_d i_q) \tag{8}$$

$$q_{Lo} = q_{\text{inv\_out}} - q_{L_f} \tag{9}$$

$$q_{Co} = q_{Lo} - q_{C_f} \tag{10}$$

where

$$q_{L_f} = \frac{3}{2}\left(\omega L_f |i_{dq}|^2 - L_f(\dot{i}_d i_q - \dot{i}_q i_d)\right)$$

$$q_{C_f} = -\frac{3}{2}\left(\omega C_f |v_{cdq}|^2 - C_f(\dot{v}_{cd} v_{cq} - \dot{v}_{cq} v_{cd})\right)$$

and each subscript has the same meaning as in the case of instantaneous real power.

Fig. 3 shows how power varies in the circuit shown in Fig. 2. Fig. 3(a) and (c) shows the instantaneous real and imaginary power at each terminal, Fig. 3(b) shows p_{Lf} and p_{Cf}, and Fig. 3(d) shows q_{Lf} and q_{Cf}. In Fig. 2, v_{inv} is a source voltage which is ideally sinusoidal. The amplitude and frequency are 220 V and 60 Hz, respectively. Neither the capacitor voltage nor the inverter output current is controlled. The left-hand side of Fig. 3 shows the transient state when resistive loads are changed abruptly from 20 to 10 Ω, and the right-hand side

shows instantaneous power variations in the steady state when the diode rectifier loads, which have a series L filter of 4.7 mH, a C filter of 1650 μF, and R of 40 Ω, are connected at the LC filter output terminal. L_f and C_f are 800 μH and 75 μF, respectively.

We note that there exist differences in instantaneous power between the input and output terminals of the LC filters in the transient state. The quicker the d–q-axis inverter output currents return to steady state, the faster p_{Lf} comes to be zero, because p_{Lf} is the function of the d–q-axis inverter output currents and current variations. The case of p_{Cf} is the same as that of p_{Lf}. The q_{Lf} is the reactive power consumed by L_f in steady state, but it is also the function of the d–q-axis inverter output currents and current variations in transient state. The case of q_{Cf} is similar with that of q_{Lf}. When a nonlinear load is applied, harmonics exist in both the inverter output current and the capacitor voltage. Because of such harmonics, the d–q-axis inverter output currents and d–q-axis capacitor voltages vary continuously. Consequently, p_{Lf}, p_{Cf}, q_{Lf}, and q_{Cf} fluctuate as well. The larger the variation in the d–q-axis inverter output currents and capacitor voltages, the bigger the difference in the instantaneous power at each terminal. Therefore, it is necessary to include the instantaneous power variation in the LC filters for more precise modeling of the UPS system.

C. Nonlinear Modeling of Systems

Expressing the real and imaginary power balances between the input and output terminals of the LC filters

$$p_{\text{inv\_out}} - p_{L_f} - p_{C_f} = \frac{3}{2}(v_{cd}i_{ld} + v_{cq}i_{lq}) \tag{11}$$

$$q_{\text{inv\_out}} - q_{L_f} - q_{C_f} = \frac{3}{2}(v_{cq}i_{ld} - v_{cd}i_{lq}). \tag{12}$$

Now, define p_f and q_f as

$$p_f = \frac{2}{3}(p_{\text{inv\_out}} - p_{L_f} - p_{C_f}) \tag{13}$$

$$q_f = \frac{2}{3}\Bigg(q_{\text{inv\_out}} + \frac{3}{2}\left(L_f(\dot{i}_d i_q - \dot{i}_q i_d)\right. \left. - C_f(\dot{v}_{cd}v_{cq} - \dot{v}_{cq}v_{cd})\right)\Bigg). \tag{14}$$

The values p_f and q_f are calculated with measured voltages and currents, and then their ripple components are eliminated with low-pass filters for stable differentiation. From (11) and (12)

$$p_f = v_{cd}i_{ld} + v_{cq}i_{lq} \tag{15}$$

and from (12) and (14)

$$q_f = v_{cq}i_{ld} - v_{cd}i_{lq} - \omega C_f|v_{cdq}|^2 + \omega L_f|i_{dq}|^2. \tag{16}$$

Solving (15) and (16) simultaneously for i_{ld} and i_{lq}, we find

$$i_{ld} = \frac{p_f v_{cd} + q_f v_{cq}}{\left(v_{cd}^2 + v_{cq}^2\right)} + \omega\, C_f v_{cq} - \frac{\omega L_f\left(i_d^2 + i_q^2\right)}{\left(v_{cd}^2 + v_{cq}^2\right)} v_{cq} \tag{17}$$

$$i_{lq} = \frac{p_f v_{cq} - q_f v_{cd}}{\left(v_{cd}^2 + v_{cq}^2\right)} - \omega\, C_f v_{cd} + \frac{\omega L_f\left(i_d^2 + i_q^2\right)}{\left(v_{cd}^2 + v_{cq}^2\right)} v_{cd}. \tag{18}$$

Finally, substituting (17) and (18) into (3) and (4), we can write a nonlinear model of the UPS inverter as

$$\begin{bmatrix} \dot{i}_d \\ \dot{i}_q \\ \dot{v}_{cd} \\ \dot{v}_{cq} \end{bmatrix} = \begin{bmatrix} \omega i_q - \frac{1}{L_f} v_{cd} \\ -\omega i_d - \frac{1}{L_f} v_{cq} \\ \frac{1}{C_f} i_d - \frac{p_f}{C_f\left(v_{cd}^2+v_{cq}^2\right)} v_{cd} - \frac{q_f - \omega L_f\left(i_d^2+i_q^2\right)}{C_f\left(v_{cd}^2+v_{cq}^2\right)} v_{cq} \\ \frac{1}{C_f} i_q - \frac{p_f}{C_f\left(v_{cd}^2+v_{cq}^2\right)} v_{cq} + \frac{q_f - \omega L_f\left(i_d^2+i_q^2\right)}{C_f\left(v_{cd}^2+v_{cq}^2\right)} v_{cd} \end{bmatrix} + \begin{bmatrix} \frac{1}{L_f} & 0 \\ 0 & \frac{1}{L_f} \\ 0 & 0 \\ 0 & 0 \end{bmatrix} \begin{bmatrix} v_d \\ v_q \end{bmatrix} \tag{19}$$

where we have included an instantaneous power balance between the input and output terminals of LC filters, which can improve the dynamic response.

III. Design of Nonlinear Controller

A nonlinear state equation for a MIMO system is

$$\dot{x} = f(x) + gu \tag{20}$$

and the output is of that system given as

$$y = h(x). \tag{21}$$

Equation (19) is in the same form as (20), so the variables in (20) and (21) can be expressed as the transpose of row vectors as follows:

$$\begin{aligned} x &= [\,x_1 \quad x_2 \quad x_3 \quad x_4\,]^{\mathrm{T}} = [\,i_d \quad i_q \quad v_{cd} \quad v_{cq}\,]^{\mathrm{T}} \\ g &= \begin{bmatrix} 0 & g_2 & 0 & 0 \\ g_1 & 0 & 0 & 0 \end{bmatrix}^{\mathrm{T}} = \begin{bmatrix} 0 & 1/L_f & 0 & 0 \\ 1/L_f & 0 & 0 & 0 \end{bmatrix}^{\mathrm{T}} \\ u &= [\,u_1 \quad u_2\,]^{\mathrm{T}} = [\,v_d \quad v_q\,]^{\mathrm{T}} \\ y &= [\,y_1 \quad y_2\,]^{\mathrm{T}} = [\,v_{cd} \quad v_{cq}\,]^{\mathrm{T}}. \end{aligned}$$

One method of input–output feedback linearization for the nonlinear model begins by differentiating the output until the input appears. The result is

$$\begin{bmatrix} \ddot{y}_1 \\ \ddot{y}_2 \end{bmatrix} = \begin{bmatrix} A_1(x) \\ A_2(x) \end{bmatrix} + \begin{bmatrix} E_{11}(x) & E_{12}(x) \\ E_{21}(x) & E_{22}(x) \end{bmatrix} \begin{bmatrix} u_1 \\ u_2 \end{bmatrix}. \tag{22}$$

A detailed derivation of this is provided in [9].

If the decoupling matrix $E(x)$ is nonsingular in all operation ranges, a control law is obtained from (22) as

$$\begin{bmatrix} u_1 \\ u_2 \end{bmatrix} = \begin{bmatrix} \hat{E}_{11}(x) & \hat{E}_{12}(x) \\ \hat{E}_{21}(x) & \hat{E}_{22}(x) \end{bmatrix} \left[- \begin{bmatrix} A_1(x) \\ A_2(x) \end{bmatrix} + \begin{bmatrix} v_1 \\ v_2 \end{bmatrix} \right] \tag{23}$$

where

$$\begin{bmatrix} \hat{E}_{11}(x) & \hat{E}_{12}(x) \\ \hat{E}_{21}(x) & \hat{E}_{22}(x) \end{bmatrix} = \begin{bmatrix} E_{11}(x) & E_{12}(x) \\ E_{21}(x) & E_{22}(x) \end{bmatrix}^{-1}$$

and v_1 and v_2 are the outputs of linear controllers, which are the new control inputs for the linearized system.

Equation (22) depicts the plant, and (23) represents the control part, respectively, as shown in Fig. 4(a). Substituting (23) into (22), a nonlinearity of the system is cancelled, which

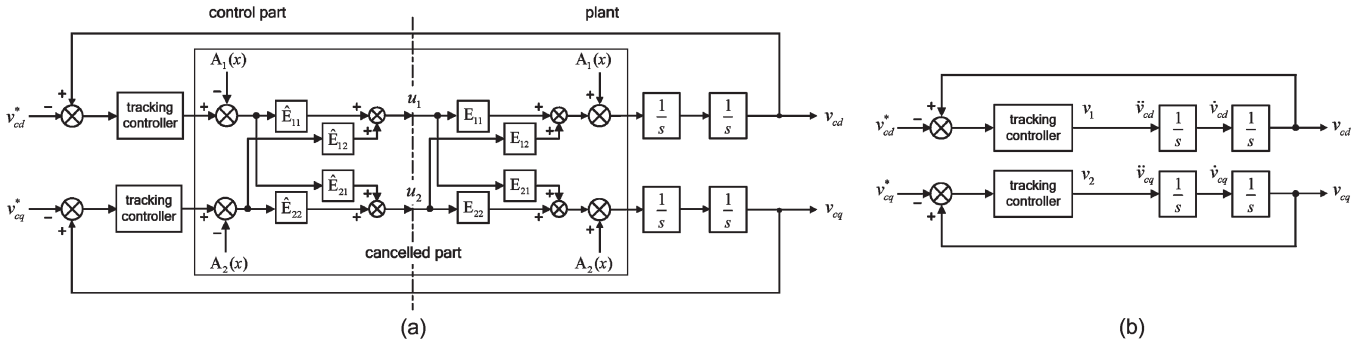

Fig. 4. Feedback linearization control for UPS inverters with LC filters. (a) Full block diagram. (b) Simplified block diagram.

results in a simple linearized system consisting of double integrators with a linear tracking controller, as shown in Fig. 4(b).

In the design of the tracking controller, the integral controller is added to eliminate the steady state error due to parameter variations [10], [20], [21] as follows:

$$\begin{bmatrix} v_1 \\ v_2 \end{bmatrix} = \begin{bmatrix} \ddot{y}_{1\mathrm{ref}} - k_{11}\dot{e}_1 - k_{12}e_1 - k_{13}\int e_1 dt \\ \ddot{y}_{2\mathrm{ref}} - k_{21}\dot{e}_2 - k_{22}e_2 - k_{23}\int e_2 dt \end{bmatrix} \tag{24}$$

where $e_1 = y_1 - y_{1\mathrm{ref}}$ and $e_2 = y_2 - y_{2\mathrm{ref}}$. If the all gains of $k_{11}(k_{21})$, $k_{12}(k_{22})$, and $k_{13}(k_{23})$ are positive, the tracking error converges to zero.

As shown in Fig. 4(b), the closed-loop transfer function of the d-axis tracking controller and the d-axis plant can be represented as

$$T_d(s) = \frac{k_{11}s^2 + k_{12}s + k_{13}}{s^3 + k_{11}s^2 + k_{12}s + k_{13}}. \tag{25}$$

The closed-loop transfer function of the q-axis tracking controller and the q-axis plant is similar to the function in (25). The poles of this transfer function are s_1, s_2, s_3, which can be chosen on the negative real axis by the controller gains. Thus, the gains of tracking controller are $k_{11}(k_{21}) = -(s_1 + s_2 + s_3)$, $k_{12}(k_{22}) = s_1 \cdot s_2 + s_2 \cdot s_3 + s_3 \cdot s_1$, $k_{13}(k_{23}) = -s_1 \cdot s_2 \cdot s_3$. Thereby, in this paper, the poles are chosen as $s_1 = -100$, $s_2 = s_3 = -4500$ by trial-and-error method.

IV. Experimental Results

To verify the validity of the proposed control algorithm, we carried out experiments for the linear load (R 10 Ω, L 3.5 mH) and the nonlinear load (diode rectifier of Fig. 2—L 4.7 mH, C 1650 μF, R 40 Ω).

In our experiment, we used the three-phase ac/dc/ac insulated-gate-bipolar-transistor pulsewidth-modulation converter with dc-link capacitors. The rated voltage and frequency are 220 V and 60 Hz, respectively. The dc-link voltage is controlled at 360 V, and the switching frequency of both converters is 9 kHz. The cutoff frequency of the LC filters is chosen to be 650 Hz, hence the filter inductor L_f is 800 μH and the filter capacitor C_f is 75 μF.

The gain selection for each of controllers is shown in the Table I. The design method for the PI controller is described in [22]. Fig. 5 shows the transient responses of the output voltage in the case of applying RL loads abruptly from no load. For the conventional PI controller (henceforth "PI"),

TABLE I
Parameters of Controllers

Controller	Gains of controllers	
PI controller	Inverter output current controller (inner loop) ($\omega_i = 12000$) : ω_i is chosen a fifth times the switching frequency.	
	P controller	$\omega_i \cdot L_f = 9.6$
	I controller	$\omega_i \cdot 0.01 = 120$
	Inverter output voltage controller (outer loop) ($\xi = 0.707$, $\omega_v = 2500$) : ω_v is chosen a fifth times ω_i	
	P controller	$2 \cdot \xi \cdot \omega_v \cdot C_f = 0.265125$
	I controller	$\omega_v^2 \cdot C_f = 468.75$
FL-SISO	PI controller	Inner loop: the same as above Outer loop: the same as above
	Nonlinear controller	k_1: 9.1×10^3 k_2: 2.115×10^7 k_3: 2.025×10^9
FL-MIMO	Nonlinear controller	$k_{11(21)}$: 9.1×10^3 $k_{12(22)}$: 2.115×10^7 $k_{13(23)}$: 2.025×10^9

Fig. 5(a) shows the slow transient response. The PI controller with compensation for the load current in the feedforward type ("PI-FC") gives the fast transient response shown in Fig. 5(b). However, this method has the disadvantage that it requires additional load current sensors for feedforward compensation of load currents. Fig. 5(c) shows the transient response with the feedback linearization control ("FL-SISO") that regulates only the capacitor q-axis voltage, where the d-axis voltage is controlled with separate PI controllers. The design method for FL-SISO is described fully in [9]. Fig. 5 shows the performance of the proposed feedback linearization control ("FL-MIMO"). As can be seen, there are no significant differences between the methods except the "PI" control.

Fig. 6 shows the same waveforms as in Fig. 5, with the nonlinear load consisting of a diode rectifier, as shown in Fig. 2. In Fig. 6(a), the d–q-axis voltages contain high ripple components, and the sinusoidal waveform is much distorted. Fig. 6(b) shows a good performance. In Fig. 6(c), the q-axis voltage is good, but the d-axis voltage contains high ripple components, similar to Fig. 6(a). In Fig. 6(d), the FL-MIMO gives a good performance, similar to Fig. 6(b).

Table II provides a comparison of the THD factor for the different cases. Even though FL-MIMO has slightly high THD

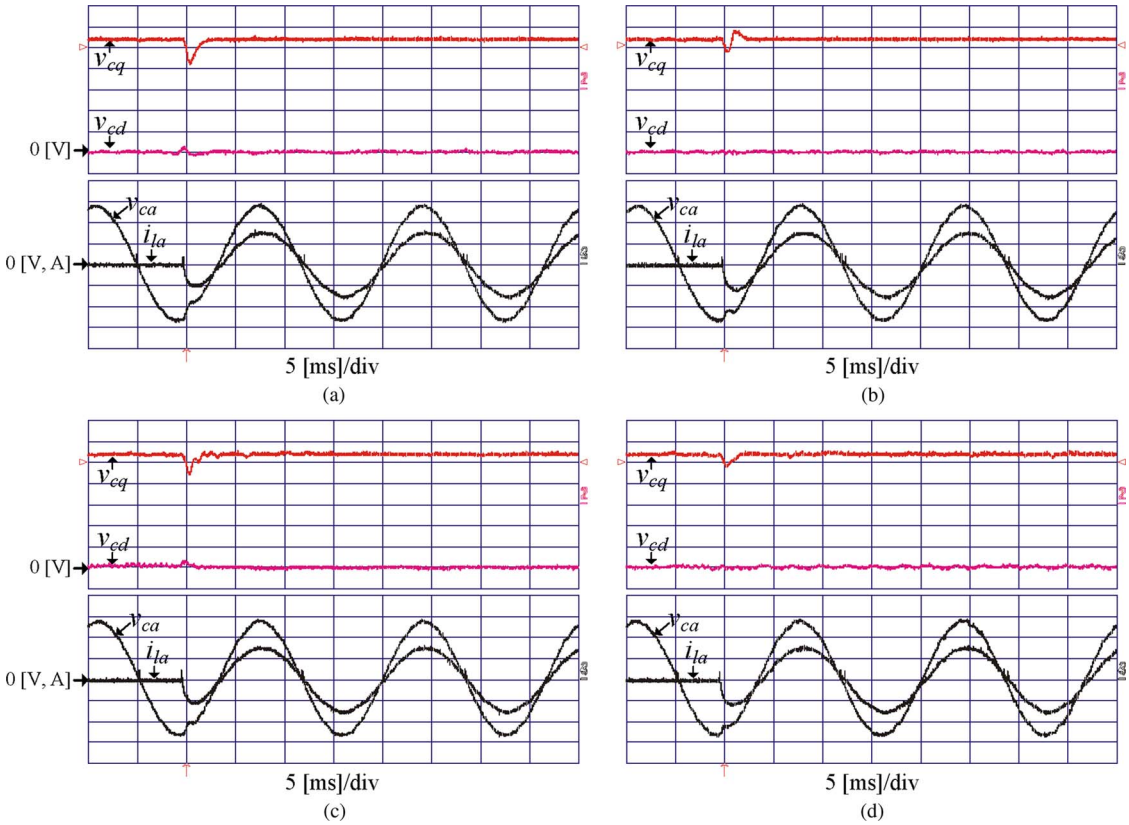

Fig. 5. Transient responses to impact loading of RL from no load (v_{cd}, v_{cq}: 34 V/div, v_{ca}: 68 V/div, i_{la}: 12 A/div). (a) PI. (b) PI-FC. (c) FL-SISO. (d) FL-MIMO (proposed).

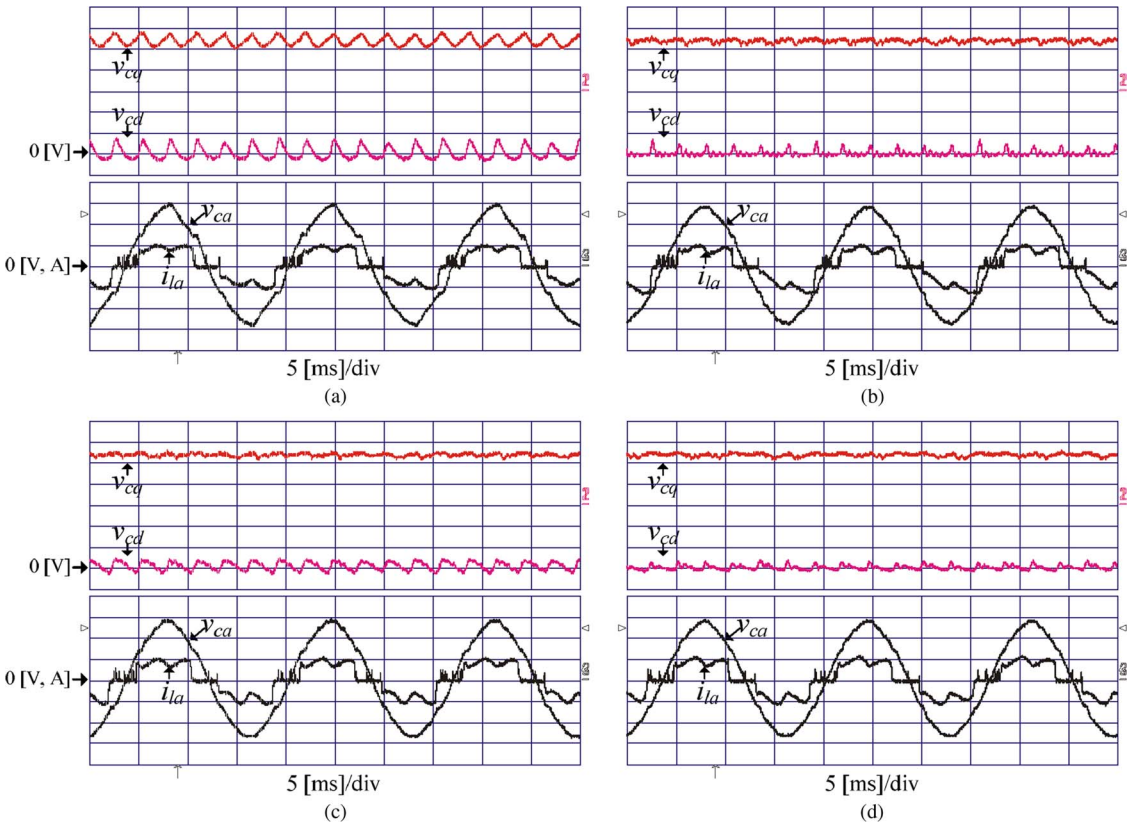

Fig. 6. Control performance at nonlinear load (diode rectifier) (v_{cd}, v_{cq}: 34 V/div, v_{ca}: 68 V/div, i_{la}: 9 A/div). (a) PI. (b) PI-FC. (c) FL-SISO. (d) FL-MIMO (proposed).

TABLE II
ANALYSIS OF THD

Controller type	THD	
	RL load	Diode rectifier
PI controller (PI)	0.32 %	5.86%
PI with feed-forward (PI-FC)	0.27 %	1.78%
Feedback linearization (FL-SISO)	0.31 %	3.52%
Feedback linearization (FL-MIMO)	0.57%	1.85%

values because of the differential components [10] in $A(x)$ which is compensated for feedback linearization, as shown in Fig. 4, the THD factors for RL loads are very low in all the controllers. For nonlinear loads, however, the PI and FL-SISO controllers give high THD values, and the PI-FC and FL-MIMO give lower values of THD, less than 1.9%.

V. CONCLUSION

In this paper, we have proposed a novel output voltage control scheme for UPS systems using multivariable feedback linearization. A UPS inverter system has been modeled as a nonlinear system by applying instantaneous power balance between the input and the output terminals of the LC filters. By using the feedback linearization technique, we linearized the nonlinear model, of which the controller was designed with the linear control theory. The validity of the proposed scheme (FL-MIMO) was verified by experimental results, which showed that it had a better performance than the conventional method, particularly for nonlinear load, while it does not need additional load current sensors.

REFERENCES

[1] H. Tao, J. L. Duarte, and M. A. M. Hendrix, "Line-interactive UPS using a fuel cell as the primary source," *IEEE Trans. Ind. Electron.*, vol. 55, no. 8, pp. 3012–3021, Aug. 2008.

[2] J.-D. Park, C. Kalev, and H. F. Hofmann, "Control of high-speed solid-rotor synchronous reluctance motor/generator for flywheel-based uninterruptible power supplies," *IEEE Trans. Ind. Electron.*, vol. 55, no. 8, pp. 3038–3046, Aug. 2008.

[3] G. Iwanski and W. Koczara, "DFIG-based power generation system with UPS function for variable-speed applications," *IEEE Trans. Ind. Electron.*, vol. 55, no. 8, pp. 3047–3054, Aug. 2008.

[4] T. Kawabata, T. Miyashita, and Y. Yamamoto, "Dead beat control of three phase PWM inverter," *IEEE Trans. Power Electron.*, vol. 5, no. 1, pp. 21–28, Jan. 1990.

[5] U. Burup, P. N. Enjeti, and F. Blaabjerg, "A new space-vector-based control method for UPS systems powering nonlinear and unbalanced loads," *IEEE Trans. Ind. Appl.*, vol. 37, no. 6, pp. 1864–1870, Nov./Dec. 2001.

[6] Y.-Y. Tzou, S.-L. Jung, and H.-C. Yeh, "Adaptive repetitive control of PWM inverters for very low THD AC-voltage regulation with unknown loads," *IEEE Trans. Power Electron.*, vol. 14, no. 5, pp. 973–981, Sep. 1999.

[7] P. C. Loh, M. J. Newman, D. N. Zmood, and D. G. Holmes, "A comparative analysis of multiloop voltage regulation strategies for single and three-phase UPS systems," *IEEE Trans. Power Electron.*, vol. 18, no. 5, pp. 1176–1185, Sep. 2003.

[8] M. Liserre, R. Teodorescu, and F. Blaabjerg, "Stability of photovoltaic and wind turbine grid-connected inverters for a large set of grid impedance values," *IEEE Trans. Power Electron.*, vol. 21, no. 1, pp. 263–272, Jan. 2006.

[9] D.-C. Lee and J.-I. Jang, "Output voltage control of PWM inverters for stand-alone wind power generation systems using feedback linearization," in *Conf. Rec. IEEE IAS Annu. Meeting*, 2005, pp. 1626–1631.

[10] D.-E. Kim and D.-C. Lee, "Inverter output voltage control of three-phase UPS systems using feedback linearization," in *Proc. IEEE IECON*, Taipei, Taiwan, 2007, pp. 1737–1742.

[11] G. Escobar, P. Mattavelli, A. M. Stankovic, A. A. Valdez, and J. Leyva-Ramos, "An adaptive control for UPS to compensate unbalance and harmonic distortion using a combined capacitor/load current sensing," *IEEE Trans. Ind. Electron.*, vol. 54, no. 2, pp. 839–847, Apr. 2007.

[12] H. Deng, R. Oruganti, and D. Srinivasan, "A simple control method for high-performance UPS inverters through output-impedance reduction," *IEEE Trans. Ind. Electron.*, vol. 55, no. 2, pp. 888–898, Feb. 2008.

[13] S. B. Dewan, "Optimum input and output filters for a single phase rectifier power supply," *IEEE Trans. Ind. Appl.*, vol. IA-21, no. 3, pp. 282–288, May 1981.

[14] P. Cortés, G. Ortiz, J. I. Yuz, J. Rodríguez, S. Vazquez, and L. G. Franquelo, "Model predictive control of an inverter with output LC filter for ups applications," *IEEE Trans. Ind. Electron.*, vol. 56, no. 6, pp. 1875–1883, Jun. 2009.

[15] W. K. Min, J. S. Kim, and J. H. Choi, "Output LC filter design of single phase voltage source inverter used for uninterruptible power supply," *Trans. KIEE*, vol. 56P, no. 2, pp. 83–89, Jun. 2007.

[16] M. M. Malinowski and S. S. Bernet, "A simple voltage sensorless active damping scheme for three-phase converters with LCL filters," *IEEE Trans. Ind. Electron.*, vol. 55, no. 4, pp. 1876–1880, Apr. 2008.

[17] N. Mendalek, K. Al-Haddad, F. Fnaiech, and L. A. Dessaint, "Nonlinear control technique to enhance dynamic performance of a shunt active power filter," *Proc. Inst. Elect. Eng.—Elect. Power Appl.*, vol. 150, no. 4, pp. 373–379, Jul. 2003.

[18] L. Yacoubi, K. Al-Haddad, L.-A. Dessaint, and F. Fnaiech, "Linear and nonlinear control techniques for a three-phase three-level NPC boost rectifier," *IEEE Trans. Ind. Electron.*, vol. 53, no. 6, pp. 1908–1918, Dec. 2006.

[19] H. Akagi, E. H. Watanabe, and M. Aredes, *Instantaneous Power Theory and Applications to Power Conditioning*. Piscataway, NJ: IEEE Press, 2007, pp. 41–104.

[20] D.-C. Lee, G.-M. Lee, and K.-D. Lee, "DC-bus voltage control of three-phase AC/DC PWM converters using feedback linearization," *IEEE Trans. Ind. Appl.*, vol. 36, no. 3, pp. 826–833, May/Jun. 2000.

[21] D.-E. Kim and D.-C. Lee, "Feedback linearization control of grid-interactive PWM converters with LCL filters," *J. Power Electron.*, vol. 9, no. 2, pp. 288–299, Mar. 2009.

[22] J.-I. Jang and D.-C. Lee, "High performance control of three-phase PWM converters under non-ideal source voltage," in *Proc. IEEE ICIT*, Mumbai, India, 2006, pp. 2791–2796.

Dong-Eok Kim (S'07) received the B.S. and M.S. degrees in electrical engineering from Yeungnam University, Gyeongbuk, Korea, in 2005 and 2008, respectively. He is currently working toward the Ph.D. degree in electrical engineering at the University of Washington, Seattle.

He was an Engineer with LG Philips LCD (LG Display) in 2005. He was a Research Engineer in the Electrical Technology Research Department, Institute of Information and Communication, Yeungnam University, in 2008. His research interests are power converter control, power quality, and fault diagnosis.

Dong-Choon Lee (M'95) received the B.S., M.S., and Ph.D. degrees in electrical engineering from Seoul National University, Seoul, Korea, in 1985, 1987, and 1993, respectively.

From 1987 to 1988, he was a Research Engineer with Daewoo Heavy Industry. Since 1994, he has been a faculty member in the Department of Electrical Engineering, Yeungnam University, Gyeongbuk, Korea, where he is currently a Full Professor and Vice-Dean of Academic Affairs in the College of Engineering. He serves as Publication Editor of the *Journal of Power Electronics*, the Korean Institute of Power Electronics, Korea. He was a Visiting Scholar in the Power Quality Laboratory, Texas A&M University, College Station, in 1998; at the Electrical Drive Center, University of Nottingham, Nottingham, U.K., in 2001; and at the Wisconsin Electric Machines and Power Electronic Consortium, University of Wisconsin, Madison, in 2004. His research interests include ac machine drives, control of power converters, wind power generation, and power quality.